

More is Better: A Database for Spontaneous Micro-Expression with High Frame Rates

Sirui Zhao, Huaying Tang, Xinglong Mao, Shifeng Liu, Hanqing Tao, Hao Wang, Tong Xu, *Member, IEEE*, and Enhong Chen, *Senior Member, IEEE*,

Abstract—As one of the most important psychic stress reactions, micro-expressions (MEs), are spontaneous and transient facial expressions that can reveal the genuine emotions of human beings. Thus, recognizing MEs (MER) automatically is becoming increasingly crucial in the field of affective computing, and provides essential technical support in lie detection, psychological analysis and other areas. However, the lack of abundant ME data seriously restricts the development of cutting-edge data-driven MER models. Despite the recent efforts of several spontaneous ME datasets to alleviate this problem, it is still a tiny amount of work. To solve the problem of ME data hunger, we construct a dynamic spontaneous ME dataset with the largest current ME data scale, called DFME (Dynamic Facial Micro-expressions), which includes 7,526 well-labeled ME videos induced by 671 participants and annotated by more than 20 annotators throughout three years. Afterwards, we adopt four classical spatiotemporal feature learning models on DFME to perform MER experiments to objectively verify the validity of DFME dataset. In addition, we explore different solutions to the class imbalance and key-frame sequence sampling problems in dynamic MER respectively on DFME, so as to provide a valuable reference for future research. The comprehensive experimental results show that our DFME dataset can facilitate the research of automatic MER, and provide a new benchmark for MER. *DFME* will be published via <https://mea-lab-421.github.io>.

Index Terms—Emotion recognition, facial micro-expression, micro-expression recognition, datasets

1 INTRODUCTION

FACIAL expression is essential for humans to transmit emotional information, accounting for 55% of our daily communication [1]. As a particular facial expression, micro-expression (ME) usually refers to the spontaneous and subtle facial movements that appear instantaneously when an individual tries to hide or suppress real emotions under pressure. The concept of ME was first proposed in 1966 [2]. Subsequently, Ekman et al. [3] discovered a ME case in a video of a psychiatrist and depressed patient conversation in 1969. Concretely, throughout the pleasant conversation, when the psychiatrist asked the patient about her plans, a distressed expression quickly flashed across the patient's face, which was called ME by Ekman. As MEs can effectively reveal the genuine emotions of individuals, recognizing MEs can provide essential technical support in

lie detection, psychological healing, and public safety [4], [5], [6], [7].

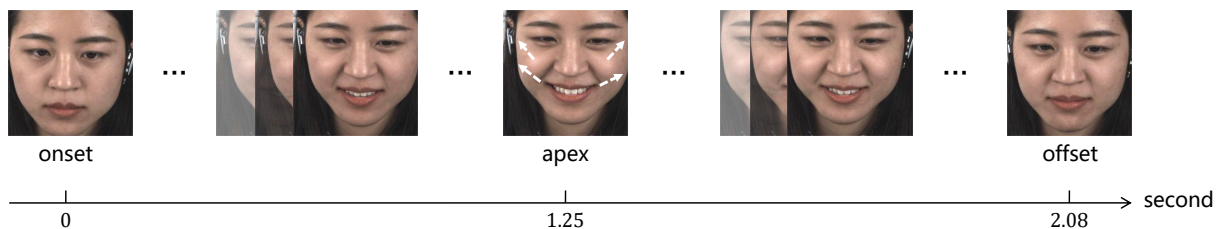
In essence, ME is a kind of psychic stress reaction. Compared with ordinary facial expression (also called macro-expression, MaE), ME has the characteristics of short duration (less than 0.5s), partial movement, and low movement intensity, so it is challenging to recognize MEs accurately. Figure 1 illustrates the comparison between a ME and a MaE with the same emotion category. It shows vividly that the MaE is obvious enough to be distinguished easily by a single image, while the ME is subtle and can only be observed through an image sequence.

The early research on ME recognition (MER) was mainly based on manual analysis in the field of psychology. However, the manual analysis relies on expert experience, which is time-consuming and labor-intensive, and has low recognition accuracy. Therefore, it is urgent to use computers' powerful perception and computing power for automatic MER. In recent years, lots of efforts in the fields of computer vision and affective computing have been devoted to automatic MER. For example, in order to extract the spatial-temporal MEs, Pfister et al. [8] introduced a local binary pattern from three orthogonal planes (LBP-TOP) [9] for MER. Liu et al. [10] proposed Mean Directional Mean Optical Flow (MDMO). Wang et al. [11] proposed Transferring Long-term Convolutional Neural Network (TLCNN). Zhao et al. [12] proposed a novel two-stage learning (i.e., prior learning and target learning) method based on a siamese 3D convolutional neural network for MER. However, due to the lack of support for a large number of well-labeled ME data, the recognition accuracy and robustness of these methods are challenging to meet the needs of actual scenarios. Therefore, it is urgent to build a large-scale ME dataset.

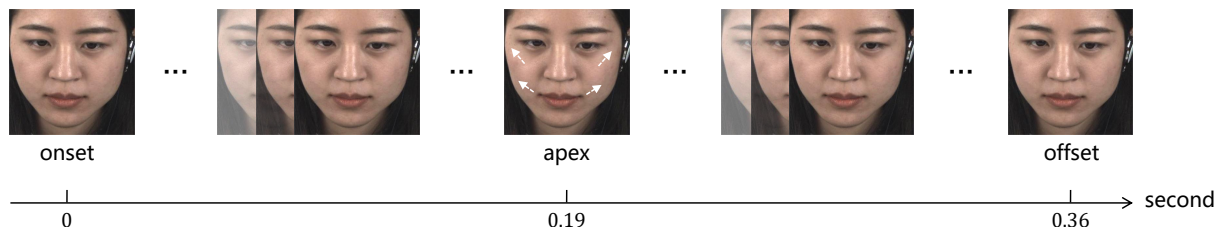
- Sirui Zhao is with the School of Computer Science and Technology, University of Science and Technology of China, Hefei, Anhui 230027, China, and also with the School of Computer Science and Technology, Southwest University of Science and Technology, Mianyang 621010, China.
E-mail: sirui@mail.ustc.edu.cn
- Huaying Tang, Hanqing Tao are with the School of Computer Science and Technology, University of Science and Technology of China, Hefei, Anhui 230027, China.
E-mail: {iamthy, hqtao}@mail.ustc.edu.cn
- Xinglong Mao, Shifeng Liu, Hao Wang, Tong Xu and Enhong Chen are with School of Data Science, University of Science and Technology of China, Hefei, Anhui 230027, China.
E-mail: {maoxl, lsf0619}@mail.ustc.edu.cn, {wanghao3, tongxu, cheneh}@ustc.edu.cn

This work has been submitted to the IEEE for possible publication. Copyright may be transferred without notice, after which this version may no longer be accessible.

Sirui Zhao, Huaying Tang, Xinglong Mao and Shifeng Liu contributed equally. Corresponding authors: Enhong Chen and Tong Xu. Manuscript received December xx, xx; revised xx xx, xx.



(a) An example of MaE with "Happiness" emotion.



(b) An example of ME with "Happiness" emotion.

Fig. 1: Examples of MaE and ME from the same person with a timeline in seconds, both belong to the "Happiness" emotion category. Noteworthy, the onset frame and the offset frame denote the start and end time of an expression respectively, and the apex frame represents the moment when an expression changes most dramatically. White arrows on the face of the apex frame indicate the general directions of facial movements, and the longer and thicker the arrows, the greater the intensity of facial movements.

Over the past decade, although researchers have published several spontaneous ME datasets, such as SMIC [13], CASME II [14], SAMM [15], MMEW [16] and CAS(ME)³ [17], these datasets have a small sample size, which still cannot completely meet the need of MER models for large-scale ME samples. In fact, building a large-scale spontaneous ME dataset is full of challenges, mainly from three aspects: First, it is difficult to induce MEs because they are facial movements that are disclosed after an individual attempts to suppress them. Second, it is difficult to label and distinguish ME fragments because the movement of ME is weak and fast, which is hard for the naked eye to perceive. Third, due to the short duration of MEs, high-speed cameras are often needed to collect them. However, the data collected by high-speed cameras are redundant, so labeling ME clips is extremely time-consuming and labor-intensive.

In order to solve the challenge of ME data shortage, this paper constructs the current largest ME dataset called DFME (Dynamic Facial Micro-expressions) to advance the development of MER. Specifically, our DFME includes 7,526 well-labeled ME videos induced by 671 participants and annotated by more than 20 annotators throughout three consecutive years. Subsequently, four popular spatiotemporal video feature learning models were reproduced on DFME to perform MER so as to objectively verify the availability of the dataset and provide a benchmark for subsequent research. In addition, aiming at the class imbalance and key-frame sequence sampling problems existing in MER, we explored different solutions to DFME. In general, the contributions of this paper could be summarized as follows:

- This paper focuses on solving the problem of lacking abundant spontaneous ME data and builds a new ME dataset called DFME containing 7,526 ME videos

across multiple high frame rates (i.e., 200fps, 300fps, 500fps). To the best of our knowledge, DFME has the largest ME sample size at present.

- We reproduced four spatiotemporal feature learning models to carry out MER tasks in DFME, objectively verifying the reliability of data quality, and providing a benchmark for subsequent MER studies.
- We explored and analyzed different solutions to the class imbalance and key-frame sequence sampling problems in dynamic MER respectively on DFME, so as to provide a reference for future research.

The rest of this paper is organized as follows. First, we summarize currently existing ME datasets and review related work on MER in the next section. In section 3, we elaborate on the building details and statistical properties of our DFME dataset. Then the comprehensive dataset evaluation is developed and discussed in Section 4. Finally, research conclusions and future work are addressed in Section 5.

2 RELATED WORK

In this section, we first review the existing public spontaneous ME datasets related to MER. Then, we summarize some representative MER studies based on deep learning technologies.

2.1 Micro-expression Datasets

The premise of obtaining an automatic MER algorithm with excellent performance is to hold a dataset with sufficient ME samples whose labels are credible and whose visual features are distinguishable. As an emerging field of affective computing, the number of ME datasets is still relatively limited.

TABLE 1: Statistical Information of Current Spontaneous ME Datasets

ME Datasets	Participants			Samples of MEs			Annotation Labels		
	Number	Gender (Male/Female)	Age	Number	Frame Rate	Resolution	Emotion	FACS AU	
SMIC	HS	16		164	100	640×480	Pos (51) Neg (70) Sur (43)		
	VIS	8	10/6	71	25	640×480	Pos (28) Neg (23) Sur (20)	No	
	NIR	8		71	25	640×480	Pos (28) Neg (23) Sur (20)		
CASME	35	22/13	Mean=22.03	195	60	640×480 1280×720	Amu (5) Dis (88) Fear (2) Con (3) Sad (6) Tense (28) Sur (20) Rep (40)	Yes	
CASME II	35	/	Mean=22.03	247	200	640×480	Hap (33) Dis (60) Sur (25) Rep (27) Oth (102)	Yes	
CAS(ME) ²	22	9/13	Range: 19-26 Mean=22.59	57	30	640×480	Pos (8) Neg (21) Sur (9) Oth (19)	Yes	
SAMM	32	16/16	Range: 19-57 Mean=33.24	159	200	2040×1088	Hap (24) Dis (8) Fear (7) Ang (20) Sur (13) Sad (3) Oth (84)	Yes	
MEVIEW	16	/	/	29	30	1280×720	Hap (5) Dis (1) Fear (3) Ang (1) Sur (8) Con(4) Unc (7)	Yes	
MMEW	36	/	Mean=22.35	300	90	1920×1080	Hap (36) Dis (72) Fear (16) Ang (8) Sur (89) Sad (13) Oth (66)	Yes	
CAS(ME) ³	PART A	100	50/50	/	943	30	1280×720	Hap (64) Dis (281) Fear (93) Ang (70) Sur (201) Sad (64) Oth (170)	Yes
	PART C	31	9/22	Mean=23.5	166	30	1280×720	Pos (16) Neg(99) Sur (30) Oth (20)	
4DME	DI4D				267	60	1200×1600		
	Grayscale	65	38/27	Range: 22-57 Mean=27.8	267	60	640×480	Pos (34) Neg (127) Sur (30) Rep (6) PosSur (13) NegSur (8) RepSur (3) PosRep(8) NegRep(7) Oth(31)	Yes
	RGB				267	30	640×480		
	Depth				267	30	640×480		
DFME	PART A	72	31/41		1118	500	1024×768	Hap (111) Dis (321) Fear (143) Ang (97) Con (77) Sur (187) Sad (142) Oth (40)	
	PART B	92	61/31	Range: 17-40 Mean=22.43	969	300	1024×768	Hap (78) Dis (406) Fear (115) Ang (56) Con (45) Sur (143) Sad (119) Oth (7)	Yes
	PART C	492	282/210		5439	200	1024×768	Hap (803) Dis (1801) Fear (634) Ang (466) Con (279) Sur (878) Sad (374) Oth (204)	

1 Some datasets contain not only MEs but also MaEs, as well as long video clips for the detection task. But here we only show the information about ME data. Note that all statistical data are from the corresponding original paper or downloaded datasets.

2 The number of participants was counted based on the data given in the corresponding original paper, but some participants were not successfully induced to make MEs.

3 Pos: Positive; Neg: Negative; Sur: Surprise; Amu: Amusement; Hap: Happiness; Dis: Disgust; Rep: Repression; Ang: Anger; Sad: Sadness; Con: Contempt; Unc: Unclear; Oth: Others; PosSur: Positively surprise; NegSur: Negatively surprise; RepSur: Repressively surprise; PosRep: Positively repression; NegRep: Negatively repression.

Nevertheless, since more and more researchers have begun to pay attention to ME analysis, some high-quality datasets are gradually springing up. Table 1 clearly summarizes the characteristics of these datasets.

As the two earliest proposed ME datasets, samples in the USF-HD [18] and Polikovskiy [19] datasets are all posed MEs. The participants were first required to watch video clips containing ME samples and then posed them by imitation. However, naturally generated MEs strongly correlate with emotions, while the posed ones are deliberately displayed and have nothing to do with the current emotional

state of the participants. Consequently, these two datasets are rarely used by researchers for ME analysis.

The subsequent researchers proposed to induce spontaneous MEs with the neutralization paradigm. Under this paradigm, several strong emotional stimuli were used to elicit expressions, during which participants were instructed to keep a neutral face as much as possible, and a certain degree of high-pressure mechanism was given to them. Datasets adopting the neutralization paradigm include SMIC [13], CASME [20], CASME II [14], CAS(ME)² [21], SAMM [15], MMEW [16], and 4DME [22], which will

be introduced in turn below.

SMIC dataset [13] is the first published spontaneous ME dataset, which consists of three parts: HS, VIS, and NIR. The HS part includes 164 ME samples from 16 participants, recorded by a high-speed camera with a frame rate of 100 frames per second (fps) and a resolution of 640×480 . Both the VIS and NIR parts contain 71 ME samples from 8 individuals, while the former part was recorded using a standard visual camera and the latter using a near-infrared camera. Two annotators classified each ME into three emotion categories (*positive*, *negative*, and *surprise*) based on the participants' self-reports about the elicitation videos. Facial action units (AUs) were not annotated in SMIC.

CASME series datasets are released by the Institute of Psychology, Chinese Academy of Sciences. As the earliest dataset in this series, CASME [20] contains a total of 195 ME samples from 19 participants with a frame rate of 60fps. Two annotators labeled the facial AUs, together with the corresponding onset, apex, and offset frames of each ME sample frame by frame. According to the facial AUs, participants' self-reports, and the relevant video content, MEs were divided into eight emotion categories: *amusement*, *sadness*, *disgust*, *surprise*, *contempt*, *fear*, *repression*, and *tense*. CASME II [14] is an advanced version of CASME. First, the number of ME samples in CASME II has been expanded to 247 samples from 26 participants. Besides, CASME II provides a higher frame rate of 200fps and facial area resolution of 280×340 to capture more subtle changes in expressions. Five emotion categories were labeled in CASME II: *happiness*, *disgust*, *surprise*, *repression*, and *others*. The CAS(ME)² dataset [21] embodies two parts, both of which were collected at 30fps and 640×480 pixels. Different from all the other datasets above, there are 87 long video clips containing both MaEs and MEs in the first part of CAS(ME)², which can be used to promote the research of ME detection. The other part consists of 300 MaEs and 57 MEs, which were labeled with four emotion tags, including *positive*, *negative*, *surprise*, and *others*.

SAMM dataset [15] has the highest resolution of all published spontaneous ME datasets, which includes 159 ME samples generated by 32 participants, with a frame rate of 200fps and a resolution of 2040×1088 . To achieve a better elicitation effect, before the formal start of the collection, participants were asked to fill in a scale, and then a series of stimulus videos were customized for each participant according to the scale. This is how SAMM differs from other datasets. SAMM contains seven emotion categories: *happiness*, *disgust*, *surprise*, *fear*, *anger*, *sadness*, and *others*. Three coders annotated the AUs and key-frames in detail for each ME sample.

MMEW dataset [16] consists of 300 ME and 900 MaE samples from 36 participants, which were collected with 90 fps and 1920×1080 resolution. Each expression sample is marked with seven emotion labels (the same as SAMM), AUs, and three key-frames. Compared with the previous datasets, MMEW is more conducive to the models using the MaE samples under the same parameter setting and elicited environment to assist in learning ME features.

To comprehensively capture the movement information of ME in all directions as much as possible, 4DME dataset [22] has made significant innovations in the record-

ing method. Each ME sample in this dataset has multi-modality video data, including 4D facial data reconstructed by 3D facial meshes sequences, traditional 2D frontal facial grayscale, RGB and depth videos. 4DME contains 267 MEs and 123 MaEs from 41 participants, thus 1,068 ME videos of four forms and 492 MaE videos in total. In addition, five emotion labels (*positive*, *negative*, *surprise*, *repression*, and *others*) were annotated based on facial AUs only, noting that each sample may have multiple emotion labels (up to two).

Unlike datasets with the neutralization paradigm, the MEVIEW dataset [23] consists of video clips of two real high-pressure scenes downloaded from the Internet. There are 29 ME samples in total, with a frame rate of 30fps and a resolution of 1280×720 , divided into seven emotion categories (the same as SAMM) with manual annotation. Although these samples are from actual life scenarios and have high ecological validity, there are many uncontrollable factors, such as frequent camera shot switching, which results in fewer segments containing full human faces.

The CAS(ME)³ dataset [17] adopted the mock crime paradigm to elicit MEs with high ecological validity. However, unlike MEVIEW, the collection was still controlled in the laboratory environment, yielding 166 MEs and 347 MaEs. CAS(ME)³ also contains two other parts: one consists of 943 MEs and 3,143 MaEs collected using the neutralization paradigm, respectively marked with AUs, key-frames, and seven emotion labels (the same as SAMM) for each sample; the other part contains 1,508 unlabeled long video clips, which can be used for the self-supervised learning task of ME detection and recognition. This dataset was collected at a frame rate of 30fps with a resolution of 1280×720 .

Despite more and more datasets striving to record the movement characteristics of MEs more detailedly and comprehensively through various methods, these datasets are still small-scale datasets. In automatic ME analysis, models based on deep learning have become mainstream by practice. However, due to the insufficient sample size, the complexity of the model can easily lead to overfitting in the training process. Though we can alleviate this problem by using data augmentation to increase the number of samples, many uncontrollable noises might be introduced. Some work has proposed using composite datasets to train the model, but different datasets have different parameter settings, and thus such a simple fusion is not reasonable. In addition, due to the short duration and low intensity of MEs, a higher frame rate may contribute to capturing more details. Nevertheless, the highest frame rate of all above datasets is only 200fps, and most are less than 100fps. Therefore, it is necessary to establish a larger-scale ME dataset with a higher frame rate.

2.2 Micro-expression Recognition Approaches

In the past decade, MER has attracted more and more attention from scholars in affective computing and computer vision. The first attempt at automatic, spontaneous MER dates back to 2011, Pfister et al. [8] utilized a local binary pattern from three orthogonal planes (LBP-TOP) to explore MER on the first spontaneous ME dataset SMIC. Since then, more and more efforts have been devoted to automatic MER. In general, the current MER methods can be

roughly divided into hand-crafted feature based and deep learning based methods. Typical hand-crafted ME features include LBP-TOP [9], HOOFF [24], 3DHOG [19], and their variants [25], [26], [27]. However, the hand-crafted feature based methods heavily rely on complex expert knowledge, and the extracted ME features have limited discrimination. Current MER methods mainly use deep neural networks for high-level expression feature learning and emotion classification, and focus on solving the challenges that ME is subtle and ME data shortage for model training. Further, according to whether the MER model considers the ME temporal information or not, we divide the current deep learning based MER methods into single frame based MER and video sequence based MER. In the following subsections, we will categorize and summarize these two types of MER methods.

2.2.1 Single frame based MER methods.

The single frame based MER method usually only uses the highest intensity frame, i.e., the apex frame with RGB or optical-flow format in the ME video, as the input of neural networks to learn the spatial ME features. After considering the challenge of lacking sufficient ME samples, Peng et al. [28] first selected ResNet-10 [29] pre-trained on a large-scale image dataset as the backbone and then continued to fine-tune the classification network on large MaE samples for MER using apex frames. Encouragingly, the recognition accuracy exceeds the hand-crafted methods based on LBP-TOP, HOOFF, and 3DHOG. Inspired by the success of capsule models on image recognition, Quang et al. [30] proposed a CapsuleNet for MER using only apex frames. Recently, Wang et al. [31] proposed an expression-identity disentangle network for MER by leveraging MaE databases as guidance. Li et al. [32] first spotted the apex frame by estimating pixel-level change rates in the frequency domain, then proposed a joint feature learning architecture coupling local and global information from the detected apex frames to recognize MEs. At the same time, Liang et al. [33] explored the effectiveness and superiority of using the optical flow of the apex frame in ME video. Inspired by this work, Liu et al. [34] first calculated the optical-flow image of the apex frame to the onset frame in the ME clips and then used the pre-trained ResNet-18 network to encode the optical-flow image for MER. In particular, they introduced domain adversarial training strategies to address the challenge of lacking large-scale ME data for training and won first place for MEGC2019. Furthermore, Zhou et al. [35] proposed a novel Feature Refinement (FR) with expression-specific feature learning and fusion for MER based on optical-flow information of apex frames. Gong et al. [36] proposed a meta-learning-based multi-model fusion network for MER.

Overall, the single frame based MER investigations are conducted on apex frames of ME videos without temporal information, which can reduce the complexity of the used deep neural networks. In addition, the single frame based MER method has the advantage of finding large-scale images for transfer learning to effectively solve the problem of model overfitting with insufficient ME data. Nevertheless, the single frame based MER discards the temporal information in the ME video, which contains rich ME clues and is an important feature that distinguishes MEs from MaEs.

2.2.2 Video sequence based MER methods.

Unlike the single frame based MER, video sequence based MER can learn spatiotemporal ME feature from the whole ME video or its sub-sequence. Thus, the video sequence based MER is preferred to the single frame based MER for providing details. After fully considering the important expression states in the ME video, Kim et al. [37] first used CNN to encode the spatial feature of each expression state (i.e., onset, onset to apex transition, apex, apex to offset transition and offset), then adopted LSTM to learn the temporal feature based on the encoded spatial ME feature. Wang et al. [11] proposed Transferring Long-term Convolutional Neural Network (TLCNN) to solve the learning of spatial-temporal ME feature under small sample ME data. The TLCNN is also based on the CNN-LSTM structure and transfers knowledge from large-scale expression data and single frames of ME video clips. Khor et al. [38] proposed an Enriched Long-term Recurrent Convolutional Network (ELRCN) that makes spatial and temporal enrichment by stacking different input data and features. Unlike the CNN-LSTM architecture, 3D convolution network (3DCNN) [39] can simultaneously learn the spatial and temporal ME features. Based on 3DCNN, Peng et al. [40] proposed a Dual Temporal Scale Convolutional Neural Network (DTSCNN), which uses the optical-flow sequences of ME videos as model input to obtain high-level ME features and can adapt to a different frame rate of ME video clips. Wang et al. [41] proposed a MER framework based on Eulerian motion based 3DCNN (EM-CED), which uses the pre-extracted Eulerian motion feature maps as input and with a global attention module to encode rich spatiotemporal information. Xia et al. [42] proposed a deep recurrent convolutional networks based MER approach, which modeled the spatiotemporal ME deformations in views of facial appearance and geometry separately. To solve the challenge of extracting high-level ME features from the training model lacking sufficient and class-balanced ME samples, Zhao et al. [12] extracted the ME optical-flow sequence to express the original ME video and proposed a novel two-stage learning (i.e., prior learning and target learning) method based on a siamese 3D convolutional neural network for MER. Sun et al. [43] proposed a knowledge transfer technique that distills and transfers knowledge from action units for MER based on crucial temporal sequences, where knowledge from a pre-trained deep teacher neural network is distilled and transferred to a shallow student neural network. Zhao et al. [44] proposed a deep prototypical learning framework on RGB key-frame sequences, namely ME-PLAN, based on a 3D residual prototypical network and a local-wise attention module for MER. Recently, with the advancement of deep learning technology, some excellent neural networks, such as GCN [45] and transformers, have also been used for MER.

Although video sequence based MER makes full use of spatial-temporal information of ME, the corresponding model has higher structural complexity and faces serious over-fitting problems on the current small-scale ME datasets. Therefore, building a large-scale ME dataset is still the primary task of developing an automatic MER system, which plays a pivotal role.

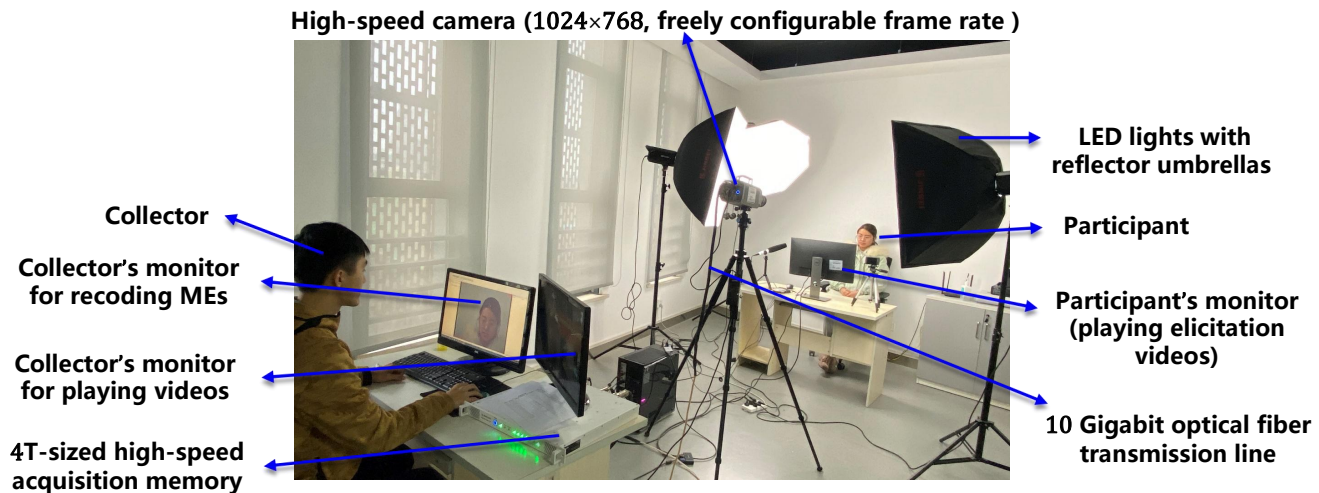


Fig. 2: Experimental environment for eliciting MEs

3 DFME

As the old saying goes, "One can't make bricks without straw". Similarly, it is difficult to design an automatic MER model with high recognition rate and reliability without sufficient training and testing samples of ME. However, due to the short-duration, low-intensity, and local-movement characteristics of ME, it is extremely challenging to construct large-scale ME datasets. To solve the problem of ME data hunger, we construct a dataset of spontaneous ME with the largest sample size at present, called DFME. In the following subsections, we will elaborate on the building details and statistical properties of our DFME dataset.

3.1 Participant and Equipment

In our DFME, 671 participants were recruited (381 males and 290 females), mainly for college students and teaching staff. Participants were age-distributed between 17 and 40 years, with a mean age of 22.43 years (standard deviation = 2.54), and all from China. Before starting the formal experiment, the participants were informed about the purpose, experimental procedure, possible benefits and risks of our research. On confirming their voluntary participation in the experiment, participants would sign an informed consent form and choose whether to allow their facial images and videos used for the academic paper.

Considering the low intensity and short duration of MEs, the recording process is easily disturbed by other factors, so it is carried out in a well-controlled laboratory environment, as shown in Fig. 2. In this environment, we set up three LED lights with reflector umbrellas to ensure a bright and stable light source on the participants' faces during experiments. In addition, we used a self-developed high-speed camera (1024×768, freely configurable frame rates) to capture MEs, and used a 10 Gigabit optical fiber transmission line to connect the camera with a 4T-sized high-speed acquisition memory to store the collected ME video clips in real-time.

3.2 Elicitation Material and Procedure

At present, there are three generations of ME-eliciting paradigms. Although the third generation has the highest

TABLE 2: Video clips for eliciting MEs

Video ID	During Time	Emotion Category	Mean Score(0-5)
02sa	3'44"	Sadness	4
03sa	4'18"	Sadness	3.36
06c	2'01"	Contempt	2.83
07a	1'26"	Anger	3.49
08su	1'26"	Surprise	2.16
09f	2'22"	Fear	3.72
10a	2'58"	Anger	4.33
11d	1'24"	Disgust	3.95
13f	2'14"	Fear	3.36
14d	1'22"	Disgust	3.23
17h	1'17"	Happiness	2.81
18h	1'58"	Happiness	3.08
20d	0'46"	Disgust	2.87
21c	1'44"	Contempt	2.11
23sa	1'44"	Sadness	3.25

ecological validity, it is inevitable to interact and have conversations with the participants when simulating the natural scenes. These irrelevant body and mouth movements caused by speaking are also a kind of noise for MEs. Therefore, we still use the neutralization paradigm to elicit MEs to avoid noise as much as possible and focus more on the movement characteristics of MEs and facilitate the operation, control, and implementation. The specific details of the elicitation process will be introduced below.

The effectiveness of elicitation materials determines the quantity and quality of MEs, so selecting the materials with high emotional valence is very crucial [14]. The stimuli we used were all video clips from the Internet, ranging in length from 46 seconds to 258 seconds. In order to find more effective stimulus materials, we recruited 50 volunteers to evaluate 30 video clips collected previously. The evaluation process was as follows: after watching each video, volunteers were asked to choose only one emotion from happiness, contempt, disgust, sadness, fear, surprise and anger as the main emotion evoked by this video, and score the stimulus level on a scale of 1 to 5, corresponding to the intensity from weakest to strongest. Finally, we took the emotion selected by more than half of the volunteers as the emotional class of each video, and by ranking the average

stimulus intensity values, we obtained the optimal 15 video clips as elicitation materials adopted in our experiment. Specific statistical details are shown in Table 2.

The collection took place in a configured laboratory environment. Before start, each participant was taken to a specific seat. By adjusting the height of the seat, the focal length of the camera and the brightness of the LED lamps, we ensured that the participant’s face appeared utterly, clearly, and brightly in the centre of the screen. Then the monitor in front of the participant would play ten randomly selected elicitation videos covering all seven basic emotional types that had been previously verified effective in turn. While watching videos, participants were required to keep a neutral face as far as possible and control the occurrence of their facial expressions. If they failed and repeatedly showed obvious expressions, they would have to complete an extraordinarily long and boring questionnaire as punishment. In addition, they were asked to keep their sitting posture upright, without excessive head movements, and devote their full attention to the video played. After watching each video, participants would have a period of rest to ease their emotions. During this procedure, they were also asked to fill in an affective grade scale according to the emotional experience generated just now, and form a self-report including the timestamp where the expression occurred, emotion category and intensity based on the video sequences recorded by the high-speed camera, which would help the subsequent annotators understand their MEs. Due to the existence of cognitive differences, the emotional orientation of the elicitation materials and the internal emotional experience of participants are sometimes not exactly consistent. What’s more, external expressions of the same emotion are also diverse on account of individual differences. Therefore, it is worth noting that requiring participants to clarify their true inner emotions when expressions appear in their self-reports is necessary.

3.3 ME Annotation

Building the DFME dataset required a two-stage annotation: the sample selection stage as well as the coding and categories labeling stage. We clipped short fragments containing valid expression samples from the collected long video sequences in the first stage. The second stage included three rounds of fine-grained annotation, through which we confirmed all MEs and labeled their key-frames, facial muscle action units (AUs), and emotion categories. Furthermore, we performed annotation agreement test to verify the reliability of emotion labels.

3.3.1 Sample Selection

In the sample selection stage, by taking a manual segmentation roughly, the video sequences collected containing participants’ facial information were segmented into several shorter video fragments containing a single or more MaEs or MEs. Using the self-developed video annotation software, an experienced annotator checked through the collected original video sequences frame by frame to locate the fragments of facial muscle movements. With the guidance of the self-reports from participants, the annotator was able to effectively distinguish whether the facial movements

were expressions definitely related to emotion, or interference data unrelated to emotion (such as violent blinking caused by dry eyelids, habitual mouth opening, etc.), and the former was retained while the latter was abandoned. Besides, we also kept some fragments with blinking or eye movements if they contained MaE or ME data.

3.3.2 Coding and Categories Labeling

After the previous sample selection stage, three rounds of fine-grained annotation were adopted successively in this stage to determine the MEs together with their three key-frames (i.e., onset frame, apex frame and offset frame), facial muscle action unit (AU) labels and emotion category labels.

The apex frame is the frame corresponding to the moment when facial expression changes most dramatically. In the first round of the fine-grained annotation, five annotators independently marked out the onset, apex, and offset frame of each expression clip, and the median value of their annotation results was determined as the final result of the three key-frames. Then we filtered the expressions whose duration from onset to offset frame was less than 500ms or from onset to apex frame was less than 250ms as the ME samples, and those out of the time limit were considered as the samples of MaEs. For instance, MEs collected at a frame rate of 500fps should meet either $f_{offset} - f_{onset} + 1 \leq 250$ or $f_{apex} - f_{onset} + 1 \leq 125$, where f_k represents the moment index corresponding to the key-frame k .

In the second round of fine-grained annotation, we mainly annotated the AUs that occurred in MEs using the Facial Action Coding System (FACS) [46]. There may exist one single AU (such as AU4) or a combination of more different AUs (for example, AU6+AU12) in a ME. When multiple categories of AUs appear, some obscure ones are easily overlooked. To enhance the reliability and integrity of the AU labels, two experienced annotators independently labeled the AUs for all the MEs identified previously. According to the actual induction of the participants during the experiments, and also referring to the AUs mainly involved in the previously published ME datasets, we totally included 24 different categories of AUs for annotation. Of these AUs, six categories appear in the upper face, 13 in the lower face, and the other five belong to miscellaneous actions. Table 3 lists the specific AU numbers and their corresponding face actions. Since the manually annotated AU intensity is highly subjective, to avoid this shortcoming, annotators merely indicated whether each AU appeared during the annotation rather than defining the intensity of its occurrence.

After labeling the AUs, the two annotators determined the final AU label through crosscheck and discussion. The reliability between the two annotators was 0.83, which was calculated as

$$R = 2 \times \frac{AU(A_1) \cap AU(A_2)}{All_{AU}} \quad (1)$$

where $AU(A_1) \cap AU(A_2)$ means the number of AUs both annotators agreed, and All_{AU} is the total number of AUs in a ME labeled out by the two annotators.

In the third round of fine-grained labeling, we performed the emotion labeling of MEs taking eight categories into

TABLE 3: Key AUs Included in DFME

Upper Face Action Units		Lower Face Action Units				Miscellaneous Actions	
AU1	Inner Brow Raiser	AU9	Nose Wrinkler	AU18	Lip Pucker	AU31	Jaw Clencher
AU2	Outer Brow Raiser	AU10	Upper Lip Raiser	AU20	Lip Stretcher	AU38	Nostril Dilator
AU4	Brow Lowerer	AU12	Lip Corner Puller	AU23	Lip Tightener	AU39	Nostril Compressor
AU5	Upper Lid Raiser	AU14	Dimpler	AU24	Lip Presser	M57	Head Forward
AU6	Cheek Raiser	AU15	Lip Corner Depressor	AU25	Lips Part	M58	Head Back
AU7	Lid Tightener	AU16	Lower Lip Depressor	AU28	Lip Suck		
		AU17	Chin Raiser				

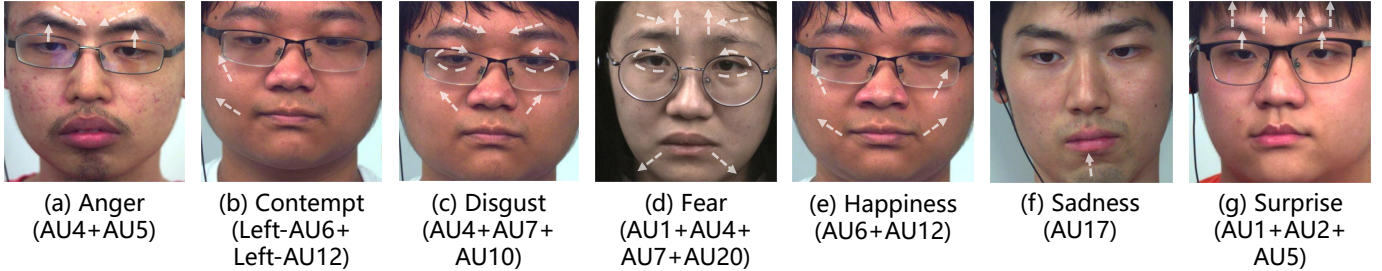


Fig. 3: Representative ME Samples of Seven Basic Emotion Categories in DFME

account: *anger, contempt, disgust, fear, happiness, sadness, surprise*, and *others*. ‘Others’ represents MEs that are difficult to divide into the former seven prototypical emotion categories. Seven annotators independently gave the emotion labels of all MEs, taking the emotion category that more than half agreed with as the final label.

In previous spontaneous ME datasets, the reference basis of emotion labeling was not precisely the same. In some datasets, as represented by SMIC, emotion labels were determined based on self-reports provided by participants. Some other studies believed that seeing is believing, so their annotation was based on the correspondence between AUs and emotions. However, on the one hand, unlike MaEs, only part of the AUs can appear simultaneously in MEs due to their low intensity, and some AUs are shared by different emotion categories, which may lead to category confusion. On the other hand, we should not ignore the differences in self-emotional cognition of different participants, which means that the self-reports given for the whole piece of elicitation materials may be rough and inaccurate. Therefore, in DFME, the emotion labels were determined through a comprehensive analysis of facial AUs, self-reports of participants, and elicitation material contents, which is consistent with the method adopted by the CASME series. It is worth mentioning that we obtained the participants’ fine-grained self-reports in the data collection process, and this is also the information that we recommend as a priority for reference when determining emotion labels. We matched the corresponding timestamps of MEs and elicitation materials through playback, enabling participants to report their emotions for each time of successful ME induction, which significantly improved the confidence of self-reports in emotion labeling. Fig.3 shows some representative ME samples of seven basic emotion categories in DFME.

3.3.3 Annotation Agreement

Having reliable emotion categories of MEs is of vital significance for a dataset. In this section, we utilized Fleiss’s

Kappa test [47] to evaluate the quality of our emotion annotation encouraged by work [48]. Fleiss’s Kappa is a measure of the agreement among three or more annotators, testing the consistency of annotation results. Therefore, we consider Fleiss’s Kappa as an excellent indicator to evaluate the reliability of emotion annotation.

In DFME, seven annotators independently labeled each ME sample based on facial AUs, an accurate self-report, and the corresponding elicitation material content. The samples were divided into eight emotion categories: {1: anger, 2: contempt, 3: disgust, 4: fear, 5: happiness, 6: sadness, 7: surprise, 8: others}. At this time, let $n = 7$ represent the total number of annotation personnel, N indicate the total number of ME video clips, $K = 8$ represent the number of emotion categories. n_{ij} is the number of annotators who assigned the i -th ME video clip to the j -th category, so we can calculate p_j , the proportion of all assignments which were to the j -th emotion:

$$p_j = \frac{1}{N \times n} \sum_{i=1}^N n_{ij}, \quad (2)$$

$$\sum_{j=1}^K p_j = 1. \quad (3)$$

Then, the extent of agreement among the n annotators for the i -th ME video clip indicated by P_i is calculated. In other words, it can be indexed by the proportion of pairs agreeing in their evaluation of the i -th ME out of all the $n(n - 1)$ possible pairs of agreement:

$$P_i = \frac{1}{n \times (n - 1)} [(\sum_{j=1}^K n_{ij}^2) - n], \quad (4)$$

The mean of P_i is therefore:

$$\bar{P} = \frac{1}{N} \sum_{i=1}^N P_i, \quad (5)$$

TABLE 4: AUs of High Occurrence in MEs of Seven Basic Emotion Categories

Anger		Contempt		Disgust		Fear		Happiness		Sadness		Surprise	
AU	pct(%) ¹	AU	pct(%)	AU	pct(%)	AU	pct(%)	AU	pct(%)	AU	pct(%)	AU	pct(%)
AU4	72.5	L/R-AU12 ²	78.7	AU4	73.6	AU4	54.1	AU12	79.8	AU4	42.2	AU1	65.6
AU7	29.1	AU6	19.2	AU7	40.4	AU7	35.3	AU6	61.6	AU14	26.1	AU5	60.2
AU24	16.3	L/R-AU10	10.6	AU10	11.8	AU5	16.2	AU24	12.1	AU24	19.2	AU2	60.0
AU5	7.6	AU7	7.8	AU24	8.4	AU24	14.5	L/R-AU12	10.1	AU7	16.5	L/R-AU2	25.6
AU23	5.6	L/R-AU2	5.7	AU14	6.7	AU1	11.1	AU10	6.2	AU17	10.8	L/R-AU1	17.8
AU14	5.6	AU14	5.7			AU14	8.8			AU15	6.9	L/R-AU5	10.7
AU10	5.2					AU17	6.0			AU23	5.1		
AU17	4.8					AU10	4.8			AU1	4.8		

¹ percentage(pct): the statistical range is all MEs from the first 300 participants.
² L/R means the Left/Right half part of an AU.

And we also have \overline{P}_e :

$$\overline{P}_e = \sum_{j=1}^K p_j^2, \quad (6)$$

Finally, we can calculate κ by:

$$\kappa = \frac{\overline{P} - \overline{P}_e}{1 - \overline{P}_e}. \quad (7)$$

Thus, we obtained $\kappa = 0.72$ through performing Fleiss’s Kappa test in DFME. According to Table 5, we know that all of our emotion annotators achieve substantial agreement, meaning that our emotion labels are quite reliable.

TABLE 5: Interpretation of κ for Fleiss’Kappa Test

κ	Interpretation
≤ 0	Poor agreement
0.01-0.20	Slight agreement
0.21-0.40	Fair agreement
0.41-0.60	Moderate agreement
0.61-0.80	Substantial agreement
0.81-1.00	Almost perfect agreement

3.4 Statistical Properties of DFME

The DFME dataset consists of three parts: PART A, PART B, and PART C. The only difference between these three parts is the frame rate setting of the high-speed camera in the experiment. In PART A, all 1,118 ME samples from 72 participants have a frame rate of 500fps. The frame rate of PART B is 300fps with 969 ME samples from 92 participants. PART C has the most data size with 5,439 ME samples from 492 participants, whose frame rate is 200fps. Although we recruited a total of 671 participants, 15 of them had strong control over their facial expressions, from whom we could not collect any ME sample. Therefore, the final DFME dataset contains 7,526 ME samples from 656 participants, and we gave each sample an emotion category label as well as AU labels annotated according to FACS. Fig.4 describes the distribution of ME samples detailedly.

Given that we have collected the fine-grained self-reports and the AU labels with considerable reliability, this is conducive to finding the emotion-AU correspondence rule in MEs. Therefore, we counted the ratio of high-occurrence AUs in each emotion (Table 4), which reflects the existence preference of AU in MEs with different emotions,

not affected by the emotional category imbalance problem in the dataset. We also matched the emotion and AU combinations according to the statistical results, and the conclusions are shown as Table 6.

TABLE 6: Matching Emotion and AU Combinations in MEs

Emotion Categories	AU Combinations
Anger	AU4+AU5, AU23
Contempt	L/R-AU12, AU6+L/R-AU12
Disgust	AU4+AU7+AU10, AU14
Fear	AU14+AU24, AU1+AU4, AU4+AU5
Happiness	AU6+AU12, AU12
Sadness	AU14, AU17, AU15, AU14+AU24
Surprise	AU1+AU2+AU5, AU1+AU2, AU5
Shared ¹	AU4, AU4+AU7, AU7, AU24

¹ Shared: the AU combinations commonly appearing in Anger, Disgust, Fear and Sadness with high frequency.

Based on the statistical results presented in Table 4, we have some findings to discuss:

- In MaEs, AU9 (nose wrinkler) is highly associated with *disgust*, and AU20 (lip stretcher) is related to *fear*. These two AUs frequently appear in MaEs but are not easily induced in MEs. We ought not to conclude that these AUs’ association with their corresponding emotions no longer exists in MEs. Instead, when participants tried to restrain their emotions, it was easier for them to control the movement of certain facial muscles such as AU9 and AU20 rather than others.
- AU4 (brow lowerer), AU7 (lid tightener), and AU24 (lip presser) simultaneously occur at high frequency in different negative emotions (*disgust*, *anger*, *fear*, *sadness*, etc.). Without the assistance of participants’ fine-grained self-reports, it is definitely challenging to distinguish MEs of negative emotions merely relying on these common AUs, which is also one of the reasons why some models excessively confuse the *disgust* MEs with those of other negative emotions in the seven-classification automatic MER task.
- In the positive emotion (*i.e.*, *happiness*), some AUs related to negative emotions can occur together with AU6 or AU12, specifically, including AU10 (associated with *disgust*), AU24 (associated with negative emotions), and Left/Right-AU12 (associated with *contempt*). The appearance of these extra AUs is a

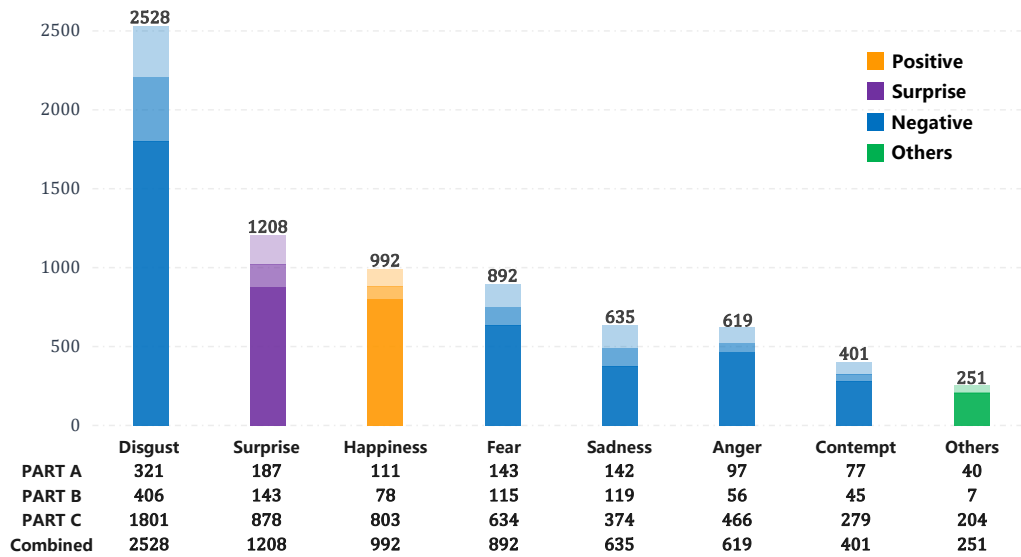


Fig. 4: Distribution of ME Samples in DFME. Each column represents the total sample number of an emotion category, and the three pieces colored from light to deep show the proportion of samples in PART A, PART B, and PART C, respectively.

sign of participants trying to suppress their positive feelings, hide their smiles and twist their expressions.

4 DATASET EVALUATION

In this section, we conducted comprehensive experiments to verify the effectiveness of our DFME dataset for automatic MER task based on influential spatiotemporal feature learning models. In addition, we specifically analyzed the class imbalance problem in ME datasets, and explored two kinds of strategies to solve the class imbalance problem in our DFME. Furthermore, we explored the influence of different sampling strategies of ME key-frame sequence on MER. These experiments can provide reference for future MER research using DFME dataset.

4.1 Evaluation Dataset

The DFME dataset is described in detail in Section 3. For the subsequent MER verification, we combined 7,275 samples with clear emotion labels in PART A, B and C of DFME as our experimental dataset. The emotion labels include *disgust*, *surprise*, *happiness*, *fear*, *sadness*, *anger* and *contempt*.

4.2 Data Preprocessing

In facial expression recognition, many variables, such as backgrounds, head poses and unequal video lengths, can affect the final recognition results. Therefore, before formally conducting automatic MER experiments, we need to preprocess all ME videos in the following steps to minimize the influence of irrelevant variables.

4.2.1 Face Alignment

To eliminate the differences in pose and angle among all ME samples, we need to perform face alignment. In this step, we took the following operations for each ME sample. We first selected a frontal face image as a reference and adopted Style Aggregated Network (SAN) [49] to extract its facial

landmarks. Afterwards, we used Procrustes analysis [50] to compute an affine transformation based on landmarks of the onset frame and landmarks of the reference image. The reason why we did not use landmarks of all frames in the ME video is to avoid errors introduced by the calculation of landmarks and transformations having a significant impact on real MEs. Finally, the transformation was operated for each frame to align the faces. Besides, some landmarks are located in regions where MEs may appear, which may not be stable enough for alignment. Thus, we excluded such landmarks when performing the alignment.

4.2.2 Face Cropping

Since the movement of MEs is mainly in the facial area, face cropping is also a necessary step to eliminate the bias caused by different backgrounds. After face alignment, we chose RetinaFace [51] to crop the faces. For reasons similar to face alignment, face cropping was based on the onset frame instead of each frame of a sample.

4.2.3 ME key-frame sequence sampling

Different ME videos have different lengths, while deep learning models usually require a fixed input size, which is shorter than ME sample lengths. Before inputting into the model, we need to normalize the temporal length of all ME videos. In general, video classification models usually adopt the uniform sampling method to unify the video length. However, this processing strategy is coarse-grained for recognizing ME with local and subtle movements. Following previous studies [12], [44] and to be compatible with popular video classification models, this work extracts 16 key-frames from each ME video based on the annotated three ME key-frames (i.e., onset frame, apex frame, and offset frame) and temporal adaptive sampling strategy [44].

4.3 Evaluation Protocols and Metrics

Due to the small sample size of previous datasets such as CASME II [14], SAMM [15], and SMIC [13], most MER stud-

ies adopted the leave-one-subject-out strategy when evaluating on them. Nevertheless, considering that the number of ME clips in DFME is relatively large, this paper put to use a simpler and more efficient 10-fold cross-validation strategy. For each fold, 10% of the data were sampled as the test set, and the remaining 90% as the training set. In addition, three commonly used MEs classification indicators, namely Accuracy, Unweighted F1-Score and Unweighted Average Recall, were used to evaluate the MER performance. Specifically, before calculating them, we need to obtain the True Positive (TP_i), False Positive (FP_i), and False Negative (FN_i) for each class i (K classes in total, and $K = 7$ in DFME). In the end, we took the average results of ten experiments as the final result.

4.3.1 Accuracy (ACC)

Accuracy is one of the most common metrics, which can evaluate the overall performance of the recognition method on the dataset. It was calculated as follows:

$$ACC = \sum_{i=1}^K \frac{TP_i}{N_i}, \quad (8)$$

where N_i is the number of samples of the i -th class.

4.3.2 Unweighted F1-score (UF1)

Unweighted F1-score (UF1), also known as macro-averaged F1-score, is defined as shown below:

$$UF1 = \frac{1}{K} \sum_{i=1}^K UF1_i, \quad (9)$$

where we have:

$$UF1_i = \frac{2 \cdot TP_i}{2 \cdot TP_i + FP_i + FN_i}. \quad (10)$$

Class imbalance is an intractable problem in the MER task, so introducing UF1 as an evaluation metric can better measure the method's performance in all classes rather than in some major classes.

4.3.3 Unweighted Average Recall (UAR)

Unweighted Average Recall (UAR) is also a more reasonable metric than accuracy in case of class imbalance.

$$UAR = \frac{1}{K} \sum_{i=1}^K \frac{TP_i}{N_i}. \quad (11)$$

Both UF1 and UAR can effectively evaluate whether MER methods give correct predictions in all classes.

4.4 Evaluation Baseline Models

Although the spatiotemporal convolution models with deeper layers and more parameters have achieved amazing performance in the video classification tasks, due to the scarcity of ME data, previous MER studies rarely use such a model with a large number of parameters. In fact, both time and space contain unique features of ME, and MER should take into account both dimensions. To verify the feasibility of applying large 3D models on our large-scale dataset and to provide a reference for backbone selection of MER methods based on extensive data, we have selected the following standard backbone networks based on 3D convolution architecture for validation experiments.

4.4.1 3D-ResNet (R3D)

Hara et al. proposed 3D-ResNet (R3D) [52] for tasks such as video classification and recognition. Since then, R3D is often used as the backbone in approaches to video-related tasks. The basic idea of this model is to replace the 2D convolutional kernels with spatiotemporal 3D kernels according to the 2D-ResNet [29] network structure.

4.4.2 Pseudo-3D ResNet (P3D)

Pseudo-3D ResNet (P3D) [53] is another 3D model backbone that has achieved good results in video tasks. It can be considered as an improved version of R3D. The key point of this model is the simulation of the $3 \times 3 \times 3$ convolution filter by using a $1 \times 3 \times 3$ spatial domain convolution filter and a $3 \times 1 \times 1$ temporal domain convolution filter. Hence the authors named it Pseudo-3D ResNet. This change controls the model size and improves training efficiency and experimental performance.

4.4.3 3D-DenseNet (D3D)

DenseNet [54] has achieved excellent performance in image tasks. It expanded the residual connection of ResNet. All layers in DenseNet connect directly with each other. 3D-DenseNet (D3D) has also been widely used in the video field. In the field of MER, Cai et al. [55] proposed a 3D-DenseNet-based method.

4.4.4 Inflated 3D ConvNet (I3D)

Inflated 3D ConvNet (I3D) [56] is based on 2D ConvNet inflation. The model size has increased significantly compared to the 2D model. Therefore, the data requirements have also increased significantly. For this reason, the authors also published a large-scale video dataset Kinetics [56] simultaneously. The results on Kinetics demonstrate the excellent performance of I3D when the amount of data is sufficient.

4.5 Evaluation Implementation Settings

Our MER experiments were all conducted on 2 NVIDIA GeForce RTX 3090 GPUs or a single NVIDIA A100-PCIE-40GB GPU. Following the original settings, the length of ME clips for all models was 16 frames, and for R3D, P3D, D3D and I3D, the sizes of each input image were 224×224 , 160×160 , 224×224 and 224×224 respectively.

During training, cross-entropy loss and stochastic gradient descent (SGD) with a momentum of 0.9 were used to optimize the model parameters, and the batch size was set to 32 for all four models. For R3D, P3D, D3D, and I3D, the initial learning rates were set to 0.005, 0.01, 0.05, and 0.005, respectively, and learning rates were divided by 10 every 10 epochs.

4.6 Evaluation Baseline Results

To demonstrate the effectiveness of our DFME dataset for automatic MER tasks, we conducted a comprehensive MER experiment based on the above four baseline models. The evaluation baseline results are shown in Table 7, and the recognition confusion matrix of each baseline model is shown in Figure 5.

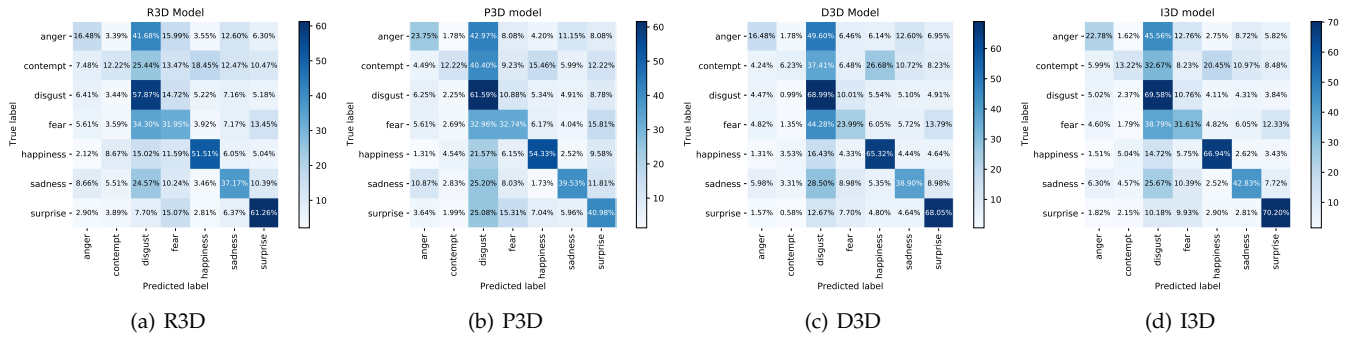


Fig. 5: Confusion matrices of R3D, P3D, D3D and I3D baseline models.

From Table 7, we can easily find that the I3D model achieved the best performance among the four backbone models with an average accuracy of 55.24%, an average UF1 of 0.4576 and an average UAR of 0.4526, and the accuracy is higher than the 47% achieved by naked eyes [57]. Besides, the other three models were approximately as accurate as the naked eye in DFME. The above experimental results demonstrate the reliability of our DFME and provided a reference for the selection of backbone models for future works. Meanwhile, by observing the recognition confusion matrices shown in Figure 5, we also find that all baseline models present the same phenomenon, that is, these models are more inclined to recognize the categories with more samples. Obviously, this is mainly caused by the class imbalance problem in DFME. Therefore, how to learn more distinguishable spatiotemporal ME features from the ME data with unbalanced classes is a vital exploration direction of MER. Besides, confusion matrices shown in Figure 5 illustrate that for all four backbone models, the *disgust* and *fear* samples are the most difficult to distinguish. This result is consistent with the statistics of the AU frequencies in Table 4. In both *disgust* and *fear* samples, the most frequent AUs are AU4 and AU7, and AU10, AU14, and AU24 are also found in both classes of samples.

TABLE 7: ME recognition performance of various baseline models

Models	ACC	UF1	UAR
R3D [52]	46.54%	0.3817	0.3827
P3D [53]	45.77%	0.3830	0.3801
D3D [55]	52.26%	0.4070	0.4107
I3D [56]	55.24%	0.4576	0.4526

4.7 Evaluation Discussion

This section will focus on two key problems that are particularly considered when using our DFME for MER, including class imbalance problem and various key-frame sequence sampling strategies.

4.7.1 Class imbalance in DFME

Since the existence of individual differences of subjects and the different inducing degrees of each category of ME, the collected spontaneous ME dataset is hard to avoid the

problem of class imbalance. This is directly reflected in the previous three datasets widely used in MER, including SMIC, CASME II and SAMM, whose ratio of the most category to the least category is 1.63, 3.52 and 6.13 [58], respectively. Inevitably the class imbalance problem still exists in our DFME dataset.

The statistic of emotion categories in DFME is shown in Table 3, from which we can find that the number of *disgust* samples is the largest among all emotion categories, accounting for about 1/3 of the proportion, and the negative samples (including *disgust*, *fear*, *sadness*, *anger* and *contempt*) accounted for about 2/3 of the proportion. Moreover, the confusion matrices in Figure 5 indicated the negative impact of class imbalance on models. All four backbone models tended to predict samples as *disgust* class more than others.

To solve the class imbalance problem, introducing a class rebalancing strategy is an effective solution. In general, the class rebalancing methods can be roughly divided into two major categories: resampling and cost-sensitive reweighting.

TABLE 8: MER Performance with and without Resampling.

Metrics	Resampling ¹	ACC	UF1	UAR
R3D	w/o	46.54%	0.3817	0.3827
	w	47.05%	0.3823	0.3659
P3D	w/o	45.77%	0.3830	0.3801
	w	42.02%	0.3949	0.4078
D3D	w/o	52.26%	0.4070	0.4107
	w	48.37%	0.4489	0.4656
I3D	w/o	55.24%	0.4576	0.4526
	w	53.91%	0.4902	0.4924

¹ w/o: without resampling, w: with resampling

Resampling is one of the most widely used class rebalancing methods. Moreover, uniform resampling is a fairly common one of all resampling strategies, which is also used in our experiments. Its main idea is to select each class of samples with an equal probability when training models, rather than sampling all samples uniformly.

Table 8 and Figure 6 show the comparison of the results with and without uniform resampling. The resampling strategy improved UAR and UF1 on the three models except for R3D, but the accuracy decreased. With the introduction of the uniform resampling strategy, the model could better learn the features of minor classes, but at the cost of weakening the ability to predict major classes correctly. How to

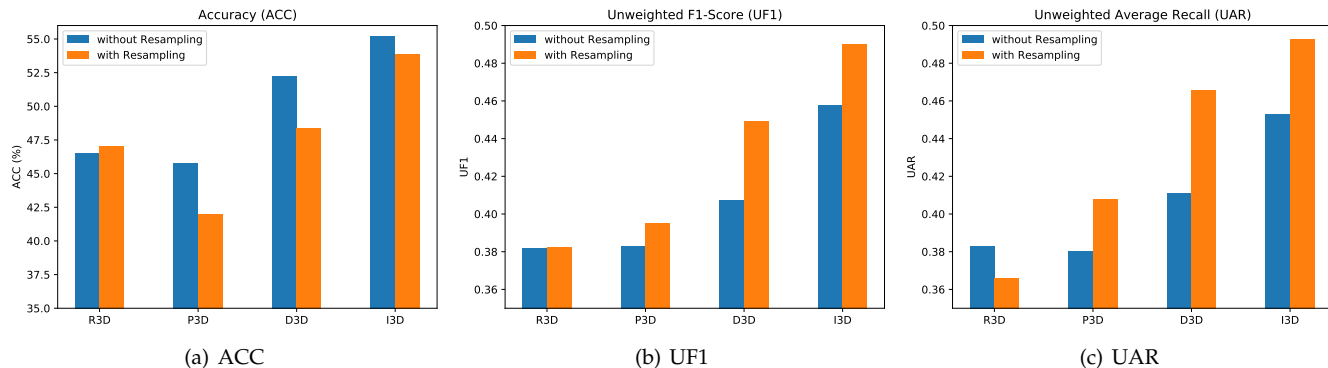


Fig. 6: Comparison of MER results with and without Resampling

reduce the information loss of the major classes in MER is a problem that needs to be addressed in future works.

Reweighting approaches attempt to rebalance different classes by reweighting their loss during training models. Class-Balanced Loss (CBLoss) [59] is a representative of reweighting loss, which is simple and effective and, therefore, used extensively in different tasks. CBLoss proposed the concept of *effective number* to estimate the actual impact of samples of each class on the model. It can also be combined with other losses, including Focal Loss [60], which reweighted samples in different classes according to their difficulty to be predicted. This feature further enhances the adaptability of CBLoss to different domains. The losses we calculated in our experiments are shown in Table 10.

The results of CBLoss are shown in Table 9. Similar to uniform resampling, CBLoss also improved the UAR and UF1 for all four models at the cost of ACC in our experiments. This result demonstrates that CBLoss is compatible with various models and suffers from similar problems as resampling. Besides, CBLoss can be easily used for different tasks with different models, but we should carefully fine-tune it in various conditions to achieve better results. In particular, the choice of β may need further study, which controls the relationship between the *effective number* and the actual number of samples.

TABLE 9: MER Performance with Different Losses

Metrics	Losses	ACC	UF1	UAR
R3D	Cross Entropy Loss	46.54%	0.3817	0.3827
	Class Balanced Loss	46.61%	0.3951	0.3914
P3D	Cross Entropy Loss	45.77%	0.3830	0.3801
	Class Balanced Loss	43.23%	0.3921	0.3955
D3D	Cross Entropy Loss	52.26%	0.4070	0.4107
	Class Balanced Loss	48.25%	0.4219	0.4302
I3D	Cross Entropy Loss	55.24%	0.4576	0.4526
	Class Balanced Loss	54.56%	0.4789	0.4777

4.8 ME key-frame sequence sampling Strategies

The key-frame sequence is a concise description of the original video, which generally contains key information about the content of the video. How to sample effective ME key-frame sequence from the raw video is also an important factor for accurate recognition of ME. Video-related

TABLE 10: Cost-Sensitive Reweighting Losses. In this table, p_y and n_y are the softmax probability and the sample number of the class y , and β is the hyperparameter in Class-Balanced Loss ($\beta = 0.999$ in our experiments).

Loss	Equation
Cross Entropy Loss	$\mathcal{L}_{ce} = -\log(p_y)$
Class-Balanced Loss [59]	$\mathcal{L}_{cb} = -\frac{1-\beta}{1-\beta^{n_y}} \log(p_y)$

recognition tasks usually adopt uniform sampling to obtain a fixed-length key-frame sequence as model input, but the instantaneously changing ME movements are often not uniformly distributed in spatial-temporal space. Previous studies [12], [44] have shown the superiority of key-frame temporal adaptive sampling based on three key moments of ME video, namely onset, apex and offset. Therefore, we hereby compare and analyze the corresponding recognition performance of these two sampling strategies (i.e., uniform sampling and temporal adaptive sampling) in DFME using baseline models.

TABLE 11: Comparison of MER Performance with Different Key-Frame Sequence Sampling Strategies.

Metrics	Sampling Method ¹	ACC	UF1	UAR
R3D	adaptive	46.54%	0.3817	0.3827
	uniform	46.49%	0.3710	0.3715
P3D	adaptive	45.77%	0.3830	0.3801
	uniform	45.31%	0.3671	0.3656
D3D	adaptive	52.26%	0.4070	0.4107
	uniform	52.62%	0.4124	0.4203
I3D	adaptive	55.24%	0.4576	0.4526
	uniform	55.21%	0.4621	0.4576

¹ adaptive: adaptive sampling in [44], uniform: uniform sampling

Table 11 and Fig 7 show the recognition performance of uniform sampling and temporal adaptive sampling [44]. It is clear that the temporal adaptive sampling strategy achieved better results on R3D and P3D models while performing worse on D3D. For I3D, the recognition performance of the two sampling strategies is comparable. This result suggests that different baseline models may require different sampling approaches.

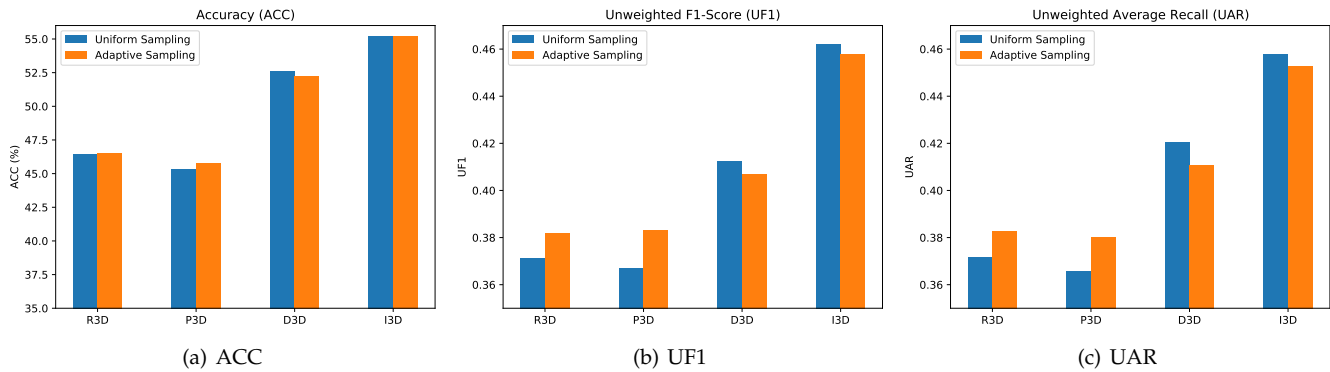


Fig. 7: Comparison of MER results of Adaptive Key-frame Sampling and Uniform Key-frame Sampling.

5 CONCLUSION AND FUTURE WORK

In this work, we focused on solving the problem of lacking abundant spontaneous ME data for MER. To this end, we built a new ME dataset called DFME containing 7,526 ME videos across multiple frame rates. To the best of our knowledge, DFME has the largest ME sample size at present. Furthermore, to verify the feasibility and validity of DFME dataset for MER task, we reproduced four spatiotemporal visual feature learning models to carry out MER task in DFME, objectively verifying the reliability of data quality, and providing a benchmark for subsequent MER studies. Particularly, we explored and analyzed two key problems when using DFME for MER, including class imbalance and key-frame sequence sampling, so as to provide directions for future MER studies using DFME.

In the future, we will strive to expand the DFME dataset to provide more abundant ME data for automatic ME analysis research, including the collection of multimodal ME data in multiple natural scenes. Based on this, we will also study the high accuracy and robust MER models, such as self-supervised MER combined with more samples with uncertain labels, and apply them to actual scenes.

ACKNOWLEDGMENTS

This work has received a lot of guidance and help from the teachers in the Micro-expression Laboratory of Institute of Psychology, Chinese Academy of Sciences. We would like to express our special thanks to them.

REFERENCES

- [1] A. Mehrabian, "Communication without words," in *Communication theory*. Routledge, 2017, pp. 193–200.
- [2] E. A. Haggard and K. S. Isaacs, "Micromomentary facial expressions as indicators of ego mechanisms in psychotherapy," in *Methods of research in psychotherapy*. Springer, 1966, pp. 154–165.
- [3] P. Ekman and W. V. Friesen, "Nonverbal leakage and clues to deception," *Psychiatry*, vol. 32, no. 1, pp. 88–106, 1969.
- [4] S. Porter and L. Ten Brinke, "Reading between the lies: Identifying concealed and falsified emotions in universal facial expressions," *Psychological science*, vol. 19, no. 5, pp. 508–514, 2008.
- [5] P. Ekman, *Telling lies: Clues to deceit in the marketplace, politics, and marriage (revised edition)*. WW Norton & Company, 2009.
- [6] S. Weinberger, "Intent to deceive? can the science of deception detection help to catch terrorists? sharon weinberger takes a close look at the evidence for it," *Nature*, vol. 465, no. 7297, pp. 412–416, 2010.
- [7] L. Hunter, L. Roland, and A. Ferozpur, "Emotional expression processing and depressive symptomatology: Eye-tracking reveals differential importance of lower and middle facial areas of interest," *Depression Research and Treatment*, vol. 2020, 2020.
- [8] T. Pfister, X. Li, G. Zhao, and M. Pietikäinen, "Recognising spontaneous facial micro-expressions," in *2011 international conference on computer vision*. IEEE, 2011, pp. 1449–1456.
- [9] G. Zhao and M. Pietikainen, "Dynamic texture recognition using local binary patterns with an application to facial expressions," *IEEE Transactions on Pattern Analysis & Machine Intelligence*, no. 6, pp. 915–928, 2007.
- [10] Y.-J. Liu, J.-K. Zhang, W.-J. Yan, S.-J. Wang, G. Zhao, and X. Fu, "A main directional mean optical flow feature for spontaneous micro-expression recognition," *IEEE Transactions on Affective Computing*, vol. 7, no. 4, pp. 299–310, 2015.
- [11] S.-J. Wang, B.-J. Li, Y.-J. Liu, W.-J. Yan, X. Ou, X. Huang, F. Xu, and X. Fu, "Micro-expression recognition with small sample size by transferring long-term convolutional neural network," *Neurocomputing*, vol. 312, pp. 251–262, 2018.
- [12] S. Zhao, H. Tao, Y. Zhang, T. Xu, K. Zhang, Z. Hao, and E. Chen, "A two-stage 3d cnn based learning method for spontaneous micro-expression recognition," *Neurocomputing*, vol. 448, pp. 276–289, 2021.
- [13] X. Li, T. Pfister, X. Huang, G. Zhao, and M. Pietikäinen, "A spontaneous micro-expression database: Inducement, collection and baseline," in *2013 10th IEEE International Conference and Workshops on Automatic face and gesture recognition (fg)*. IEEE, 2013, pp. 1–6.
- [14] W.-J. Yan, X. Li, S.-J. Wang, G. Zhao, Y.-J. Liu, Y.-H. Chen, and X. Fu, "Casm2: An improved spontaneous micro-expression database and the baseline evaluation," *PLoS one*, vol. 9, no. 1, p. e86041, 2014.
- [15] A. K. Davison, C. Lansley, N. Costen, K. Tan, and M. H. Yap, "Samm: A spontaneous micro-facial movement dataset," *IEEE transactions on affective computing*, vol. 9, no. 1, pp. 116–129, 2016.
- [16] X. Ben, Y. Ren, J. Zhang, S.-J. Wang, K. Kpalma, W. Meng, and Y.-J. Liu, "Video-based facial micro-expression analysis: A survey of datasets, features and algorithms," *IEEE transactions on pattern analysis and machine intelligence*, 2021.
- [17] J. Li, Z. Dong, S. Lu, S.-J. Wang, W.-J. Yan, Y. Ma, Y. Liu, C. Huang, and X. Fu, "Cas (me) 3: A third generation facial spontaneous micro-expression database with depth information and high ecological validity," *IEEE Transactions on Pattern Analysis and Machine Intelligence*, 2022.
- [18] M. Shreve, S. Godavarthy, D. Goldgof, and S. Sarkar, "Macro-and micro-expression spotting in long videos using spatio-temporal strain," in *2011 IEEE International Conference on Automatic Face & Gesture Recognition (FG)*. IEEE, 2011, pp. 51–56.
- [19] S. Polikovskiy, Y. Kameda, and Y. Ohta, "Facial micro-expressions recognition using high speed camera and 3d-gradient descriptor," 2009.
- [20] W.-J. Yan, Q. Wu, Y.-J. Liu, S.-J. Wang, and X. Fu, "Casm2 database: A dataset of spontaneous micro-expressions collected from neutralized faces," in *2013 10th IEEE international conference and workshops on automatic face and gesture recognition (fg)*. IEEE, 2013, pp. 1–7.
- [21] F. Qu, S.-J. Wang, W.-J. Yan, H. Li, S. Wu, and X. Fu, "Cas(me)²: a

- database for spontaneous macro-expression and micro-expression spotting and recognition," *IEEE Transactions on Affective Computing*, vol. 9, no. 4, pp. 424–436, 2017.
- [22] X. Li, S. Cheng, Y. Li, M. Behzad, J. Shen, S. Zafeiriou, M. Pantic, and G. Zhao, "4dme: A spontaneous 4d micro-expression dataset with multimodalities," *IEEE Transactions on Affective Computing*, 2022.
- [23] P. Husák, J. Cech, and J. Matas, "Spotting facial micro-expressions "in the wild"," in *22nd Computer Vision Winter Workshop (Retz)*, 2017, pp. 1–9.
- [24] R. Chaudhry, A. Ravichandran, G. Hager, and R. Vidal, "Histograms of oriented optical flow and binet-cauchy kernels on non-linear dynamical systems for the recognition of human actions," in *2009 IEEE Conference on Computer Vision and Pattern Recognition*. IEEE, 2009, pp. 1932–1939.
- [25] X. Huang, S.-J. Wang, X. Liu, G. Zhao, X. Feng, and M. Pietikäinen, "Discriminative spatiotemporal local binary pattern with revisited integral projection for spontaneous facial micro-expression recognition," *IEEE Transactions on Affective Computing*, vol. 10, no. 1, pp. 32–47, 2017.
- [26] X. Li, X. Hong, A. Moilanen, X. Huang, T. Pfister, G. Zhao, and M. Pietikäinen, "Towards reading hidden emotions: A comparative study of spontaneous micro-expression spotting and recognition methods," *IEEE transactions on affective computing*, vol. 9, no. 4, pp. 563–577, 2017.
- [27] F. Xu, J. Zhang, and J. Z. Wang, "Microexpression identification and categorization using a facial dynamics map," *IEEE Transactions on Affective Computing*, vol. 8, no. 2, pp. 254–267, 2017.
- [28] M. Peng, Z. Wu, Z. Zhang, and T. Chen, "From macro to micro expression recognition: Deep learning on small datasets using transfer learning," in *2018 13th IEEE International Conference on Automatic Face & Gesture Recognition (FG 2018)*. IEEE, 2018, pp. 657–661.
- [29] K. He, X. Zhang, S. Ren, and J. Sun, "Deep residual learning for image recognition," in *Proceedings of the IEEE conference on computer vision and pattern recognition*, 2016, pp. 770–778.
- [30] N. Van Quang, J. Chun, and T. Tokuyama, "Capsulenet for micro-expression recognition," in *2019 14th IEEE International Conference on Automatic Face & Gesture Recognition (FG 2019)*. IEEE, 2019, pp. 1–7.
- [31] B. Xia, W. Wang, S. Wang, and E. Chen, "Learning from macro-expression: a micro-expression recognition framework," in *Proceedings of the 28th ACM International Conference on Multimedia*, 2020, pp. 2936–2944.
- [32] Y. Li, X. Huang, and G. Zhao, "Joint local and global information learning with single apex frame detection for micro-expression recognition," *IEEE Transactions on Image Processing*, vol. 30, pp. 249–263, 2020.
- [33] S.-T. Liong, J. See, K. Wong, and R. C.-W. Phan, "Less is more: Micro-expression recognition from video using apex frame," *Signal Processing: Image Communication*, vol. 62, pp. 82–92, 2018.
- [34] Y. Liu, H. Du, L. Zheng, and T. Gedeon, "A neural micro-expression recognizer," in *2019 14th IEEE International Conference on Automatic Face & Gesture Recognition (FG 2019)*. IEEE, 2019, pp. 1–4.
- [35] L. Zhou, Q. Mao, X. Huang, F. Zhang, and Z. Zhang, "Feature refinement: An expression-specific feature learning and fusion method for micro-expression recognition," *Pattern Recognition*, vol. 122, p. 108275, 2022.
- [36] W. Gong, Y. Zhang, W. Wang, P. Cheng, and J. González, "Meta-mmfnet: Meta-learning based multi-model fusion network for micro-expression recognition," *ACM Transactions on Multimedia Computing, Communications, and Applications (TOMM)*, 2022.
- [37] D. H. Kim, W. J. Baddar, and Y. M. Ro, "Micro-expression recognition with expression-state constrained spatio-temporal feature representations," in *Proceedings of the 24th ACM international conference on Multimedia*. ACM, 2016, pp. 382–386.
- [38] H.-Q. Khor, J. See, R. C. W. Phan, and W. Lin, "Enriched long-term recurrent convolutional network for facial micro-expression recognition," in *2018 13th IEEE International Conference on Automatic Face & Gesture Recognition (FG 2018)*. IEEE, 2018, pp. 667–674.
- [39] S. Ji, W. Xu, M. Yang, and K. Yu, "3d convolutional neural networks for human action recognition," *IEEE transactions on pattern analysis and machine intelligence*, vol. 35, no. 1, pp. 221–231, 2012.
- [40] M. Peng, C. Wang, T. Chen, G. Liu, and X. Fu, "Dual temporal scale convolutional neural network for micro-expression recognition," *Frontiers in psychology*, vol. 8, p. 1745, 2017.
- [41] Y. Wang, H. Ma, X. Xing, and Z. Pan, "Eulerian motion based 3dcnn architecture for facial micro-expression recognition," in *International Conference on Multimedia Modeling*. Springer, 2020, pp. 266–277.
- [42] Z. Xia, X. Hong, X. Gao, X. Feng, and G. Zhao, "Spatiotemporal recurrent convolutional networks for recognizing spontaneous micro-expressions," *IEEE Transactions on Multimedia*, vol. 22, no. 3, pp. 626–640, 2019.
- [43] B. Sun, S. Cao, D. Li, J. He, and L. Yu, "Dynamic micro-expression recognition using knowledge distillation," *IEEE Transactions on Affective Computing*, 2020.
- [44] S. Zhao, H. Tang, S. Liu, Y. Zhang, H. Wang, T. Xu, E. Chen, and C. Guan, "Me-plan: A deep prototypical learning with local attention network for dynamic micro-expression recognition," *Neural networks : the official journal of the International Neural Network Society*, vol. 153, pp. 427–443, 2022.
- [45] H.-X. Xie, L. Lo, H.-H. Shuai, and W.-H. Cheng, "Au-assisted graph attention convolutional network for micro-expression recognition," *Proceedings of the 28th ACM International Conference on Multimedia*, 2020.
- [46] P. Ekman and W. V. Friesen, "Facial action coding system," *Environmental Psychology & Nonverbal Behavior*, 1978.
- [47] J. L. Fleiss, "Measuring nominal scale agreement among many raters," *Psychological bulletin*, vol. 76, no. 5, p. 378, 1971.
- [48] X. Jiang, Y. Zong, W. Zheng, C. Tang, W. Xia, C. Lu, and J. Liu, "Dfew: A large-scale database for recognizing dynamic facial expressions in the wild," in *Proceedings of the 28th ACM International Conference on Multimedia*, 2020, pp. 2881–2889.
- [49] X. Dong, Y. Yan, W. Ouyang, and Y. Yang, "Style aggregated network for facial landmark detection," pp. 379–388, 2018.
- [50] J. C. Gower, "Generalized procrustes analysis," *Psychometrika*, vol. 40, pp. 33–51, 1975.
- [51] J. Deng, J. Guo, Y. Zhou, J. Yu, I. Kotsia, and S. Zafeiriou, "Retinaface: Single-stage dense face localisation in the wild," *ArXiv*, vol. abs/1905.00641, 2019.
- [52] K. Hara, H. Kataoka, and Y. Satoh, "Can spatiotemporal 3d cnns retrace the history of 2d cnns and imagenet?" *2018 IEEE/CVF Conference on Computer Vision and Pattern Recognition*, pp. 6546–6555, 2018.
- [53] Z. Qiu, T. Yao, and T. Mei, "Learning spatio-temporal representation with pseudo-3d residual networks," *2017 IEEE International Conference on Computer Vision (ICCV)*, pp. 5534–5542, 2017.
- [54] G. Huang, Z. Liu, and K. Q. Weinberger, "Densely connected convolutional networks," *2017 IEEE Conference on Computer Vision and Pattern Recognition (CVPR)*, pp. 2261–2269, 2017.
- [55] L. Cai, H. Li, W. Dong, and H. Fang, "Micro-expression recognition using 3d densenet fused squeeze-and-excitation networks," *Appl. Soft Comput.*, vol. 119, p. 108594, 2022.
- [56] J. Carreira and A. Zisserman, "Quo vadis, action recognition? a new model and the kinetics dataset," *2017 IEEE Conference on Computer Vision and Pattern Recognition (CVPR)*, pp. 4724–4733, 2017.
- [57] M. Frank, M. Herbasz, K. Sinuk, A. Keller, and C. Nolan, "I see how you feel: Training laypeople and professionals to recognize fleeting emotions," in *The Annual Meeting of the International Communication Association. Sheraton New York, New York City*, 2009, pp. 1–35.
- [58] J. See, M. H. Yap, J. Li, X. Hong, and S.-J. Wang, "Megc 2019 – the second facial micro-expressions grand challenge," *2019 14th IEEE International Conference on Automatic Face & Gesture Recognition (FG 2019)*, pp. 1–5, 2019.
- [59] Y. Cui, M. Jia, T.-Y. Lin, Y. Song, and S. J. Belongie, "Class-balanced loss based on effective number of samples," *2019 IEEE/CVF Conference on Computer Vision and Pattern Recognition (CVPR)*, pp. 9260–9269, 2019.
- [60] T.-Y. Lin, P. Goyal, R. B. Girshick, K. He, and P. Dollár, "Focal loss for dense object detection," *2017 IEEE International Conference on Computer Vision (ICCV)*, pp. 2999–3007, 2017.



Sirui Zhao is currently working toward the PhD degree with the Department of Computer Science and Technology from University of Science and Technology of China (USTC). His research interests include automatic micro-expressions analysis, human-computer interaction (HCI) and affect computing. He has published several papers in refereed conferences and journals, including ACM Multimedia Conference, IEEE Transactions on Affective Computing, ACM TOMM, Neural Networks, etc.



Hao Wang received the PhD degree in computer science from USTC. He is currently an associate researcher with the School of Computer Science and Technology, USTC. His main research interests include data mining, representation learning, network embedding and recommender systems. He has published several papers in referred conference proceedings, such as TKDE, TOIS, NeurIPS, and AAAI..



Huaying Tang received the B.S. degree in the School of Computer Science and Technology from University of Science and Technology of China (USTC), Hefei, China, in 2021. He is currently pursuing the M.S. degree in computer science and technology in USTC. His research interests lie around automatic micro-expressions analysis and affect computing.



Xinglong Mao received the B.S degree in the School of Data Science from University of Science and Technology of China (USTC), Hefei, China. He is currently working toward the M.S. degree from the School of Data Science. His research interests include automatic micro-expressions analysis and affect computing. He has published several conference papers in ACM Multimedia Conference, etc.



Tong Xu received the Ph.D. degree in University of Science and Technology of China (USTC), Hefei, China, in 2016. He is currently working as an Associate Professor of the Anhui Province Key Laboratory of Big Data Analysis and Application, USTC. He has authored 50+ journal and conference papers in the fields of social network and social media analysis, including IEEE TKDE, IEEE TMC, IEEE TMM, KDD, AAAI, ICDM, etc.



Shifeng Liu received the B.S degree in the School of Gifted Young from University of Science and Technology of China (USTC), Hefei, China. She is currently working toward the M.S. degree from the School of Data Science. Her research interests include automatic micro-expressions analysis, human-computer interaction (HCI) and affect computing. She has published several papers in refereed conferences and journals, including ACM Multimedia Conference, Neural Networks, etc.



Enhong Chen (Senior Member, IEEE) received the PhD degree from USTC. He is a professor and vice dean with the School of Computer Science, USTC. His general area of research includes data mining and machine learning, social network analysis, and recommender systems. He has published more than 100 papers in refereed conferences and journals, including IEEE Transactions on Knowledge and Data Engineering, IEEE Transactions on Mobile Computing, KDD, ICDM, NeurIPS, and CIKM. He was on program committees of numerous conferences including KDD, ICDM, and SDM. His research is supported by the National Science Foundation for Distinguished Young Scholars of China.



Hanqing Tao is currently working toward the Ph.D. degree in the Department of Computer Science and Technology from University of Science and Technology of China (USTC). His research interests include data mining, deep learning, natural language processing and representation learning. He has published several papers in referred journals and conference proceedings, such as IEEE TKDE, IEEE TAC, AAAI, ICDM, ICME etc.